Front. Chem. Sci. Eng. 2024, 18(10): 117
https://doi.org/10.1007/s11705-024-2468-3

RESEARCH ARTICLE

Machine learning facilitated the modeling of plastics hydrothermal pretreatment toward constructing an on-ship marine litter-to-methanol plant

Yi Cheng[1,2], Qiong Pan[3], Jie Li[3], Nan Zhang[3], Yang Yang[4], Jiawei Wang (✉)[1,2], Ningbo Gao[5]

1 Department of Chemical Engineering and Applied Chemistry, Aston University, Birmingham B4 7ET, UK
2 Energy and Bioproducts Research Institute, Aston University, Birmingham B4 7ET, UK
3 Centre for Process Integration, Department of Chemical Engineering, School of Engineering, The University of Manchester, Manchester M13 9PL, UK
4 State Key Laboratory of Coal Combustion, Huazhong University of Science and Technology, Wuhan 430074, China
5 School of Energy and Power Engineering, Xi'an Jiaotong University, Xi'an 710049, China

Abstract An onboard facility shows promise in efficiently converting floating plastics into valuable products, such as methanol, negating the need for regional transport and land-based treatment. Gasification presents an effective means of processing plastics, requiring their transformation into gasification-compatible feedstock, such as hydrochar. This study explores hydrochar composition modeling, utilizing advanced algorithms and rigorous analyses to unravel the intricacies of elemental composition ratios, identify influential factors, and optimize hydrochar production processes. The investigation begins with decision tree modeling, which successfully captures relationships but encounters overfitting challenges. Nevertheless, the decision tree vote analysis, particularly for the H/C ratio, yielding an impressive R^2 of 0.9376. Moreover, the research delves into the economic feasibility of the marine plastics-to-methanol process. Varying payback periods, driven by fluctuating methanol prices observed over a decade (ranging from 3.3 to 7 yr for hydrochar production plants), are revealed. Onboard factories emerge as resilient solutions, capitalizing on marine natural gas resources while striving for near-net-zero emissions. This comprehensive study advances our understanding of hydrochar composition and offers insights into the economic potential of environmentally sustainable marine plastics-to-methanol processes.

Keywords marine plastics, hydrothermal, methanol, machine learning, techno-economic assessment

Received February 28, 2024; accepted April 14, 2024; online July 22, 2024

E-mail: j.wang23@aston.ac.uk

1 Introduction

The proliferation of plastic pollution in the oceans has led to an alarming crisis, causing devastating impacts on marine ecosystems, marine life, and human health. According to the European Parliamentary Research Service, an estimated 4.8×10^6 to 12.7×10^6 metric tons of plastic waste make their way into the oceans annually, resulting in a substantial economic cost ranging from 259 million to 695 million € [1,2]. Ocean circulation and tidal processes gather partial plastics and form gigantic ocean garbage patches [3]. The Great Pacific Garbage Patch serves as a prominent illustration of the extensive plastic accumulation in the ocean. The pressing situation urges attention and innovative strategies to tackle the ever-growing threat to the marine environment.

Several governments and organizations have dedicated themselves to addressing marine plastic pollution and arousing awareness about this pressing concern. The most well-known group, Ocean Cleanup, developed a complex continuous operating system to accumulate marine waste and enable this garbage collection [4]. However, because of seawater erosion, most plastics collected from the seas become non-recyclable or unsuitable for use, which leads to their disposal in landfills or incineration on the land [5]. The fates of the post-captured marine plastics somewhat hindered the action of ocean cleaning, particularly for some countries that banned the import of plastic waste. It is noticeable to acknowledge that marine plastic pollution is a global problem, and impractical to concentrate global waste treatment on specific lands. Hence, the on-site disposal of marine debris through a multidisciplinary collaboration in remote marine

environments, coupled with the conversion of collected plastics into valuable commodities or chemicals, emerges as a promising and scientifically robust solution for sustainably addressing this global challenge. The notion of an on-ship mobile factory, resembling a floating production storage and offloading vessel or an offshore petroleum rig, offers a compelling avenue for in situ conversion while fostering sustainability, promoting plastic waste valorization, minimizing the ecological footprint associated with cross-regional transportation, and mitigating environmental litter. This concept not only enhances its environmental friendliness but also aligns with political feasibility and profit potential, thereby harmonizing with the interests of nations in the repatriation of marine plastics.

In terms of the wastes in the marine environment, plastics account for up to 80%, and the most common constituents of marine plastics are polyethylene (PE), polystyrene, polypropylene (PP), polyamide (PA), and polyethylene terephthalate (PET) [6,7]. Low densities of polymers, such as PE and PP, with only carbon and hydrogen elements and stable C–C linkage framework chains, predominantly float on the sea and are the primary ingested plastics in the bodies of some shallow-layer creatures [8]. The deterioration from long-term insolation and seawater made them non-recyclable, and the synthesis mechanism determined hydrolysis inaccessible to create a sustainable loop through original monomers upcycling [9]. Within the spectrum of industrialized approaches for plastic conversion, syngas production stands out as a viable option to align with the concept of an on-ship mobile facility and tap into the existing well-established industrial infrastructure [10,11]. Nonetheless despite the potential of marine debris gasification, certain approaches are being explored to generate qualified syngas for accessing the industrial system. In real-world scenarios, marine debris typically consists of a mixture of polyolefins, floating polyester bottles, or PA fishing nets. The diverse and unstable nature of these materials makes their gasification challenging. Moreover, the presence of flame retardants and plasticizers can introduce additional bromine and sulfur, which significantly impact the subsequent utilization process [12,13].

Hydrothermal pretreatment (HTP) has been confirmed as an effective method for converting marine debris into a uniform gasification feedstock. It efficiently removes bromine and sulfur from heavily contaminated, moisture-laden feedstock while promoting the hydrolysis of amide and ester bonds. Consequently, this capability is well-suited for gasification pretreatment, preserving the hydrocarbon structure while breaking down polycondensation plastics like nylon and PET into smaller, soluble molecules. Raikova et al. [14] used hydrothermal liquefaction to convert marine plastics and microalgae into liquid fuels. Iñiguez et al. [15] carbonized marine plastic waste and removed all nitrogen from the feedstock in hydrothermal conditions. The increase in amide content in the liquid phase confirmed the immigration of nitrogen from solid to liquid. These findings suggest that hydrothermal could serve as a cost-effective and practical method within a highly integrated system to produce high-quality hydrochar, utilizing only water or seawater when applied to mixed buoyant plastics.

As a result, modeling the HTP to bridge the gap between the variability of marine debris and the requirement for plastic gasification is the prerequisite for customizing the attributes of each batch, ultimately guaranteeing product stability. It requires an approach to support the conditioning process by creating functional models and recognizing external influences. Machine learning (ML) is an optimal method to assist the conditioning by developing workable models and identifying foreign effects with its excellent capability for big-data analysis. Numerous studies reported using ML algorithms to investigate the thermal conversion modeling of waste plastics [16,17]. The widely explored algorithms in this area comprise decision trees (DT), random forests (RF), support vector machines (SVM), gradient boosting (GB), and neural network (NN) algorithms like artificial NN (ANN) and deep NN, and so on. For HTP of organics, researchers have predicted product yield and revealed the effect of several parameters, such as temperature, pressure, feed concentration, and reaction time [13,18]. The gradient boosting regression model well predicted R^2 values of 0.90–0.95 for the predictions of H_2, CH_4, CO_2, and CO [13]. When modeling the influence of biomass properties on hydrogen production and energy efficiency during hydrothermal gasification, four ML methods (ANN, GPR, SVM, and RF) all displayed promising predictive capability ($R^2 > 0.98$). ML approach predicted bio-oil yields and higher heating values from hydrothermal liquefaction of wet biomass and wastes with 17 input features from feedstock characteristics (biological and elemental properties) and operating conditions [19]. An extreme GB (XGB) model gave the best prediction accuracy at R^2 value of nearly 0.9 for bio-oil yields, and R^2 value of about 0.87 for higher heating values. Despite the efficiencies of the mentioned algorithms in biomass hydrothermal conversion, the complexity of the process made it challenging to explain the fundamental mechanisms and the connections between input and output because of the "black box" attribute.

To our best understanding, no previous work has proposed a conceptual on-ship facility to address marine debris. Correspondingly, assessing the feasibility of gasification digestion is a necessary investigation before transitioning a land-based facility onto a ship. Hence, within the nature of marine plastics and the conditions for gasification, this study first develops a ML model to explain plastic HTP, with modeling data from experimental data and publications with different virgin

plastics, salts, and operation parameters. The model aimed to recognize the nonlinear interactions between input and output variables, interpret explainable information and evaluate variables in a complicated data-driven model. Furthermore, based on the model established, this study selected an integrated land-based factory model as a standard to reveal the economic potential and technical feasibility of this novel idea. This work provides the understanding and evidence for future modeling and experiments to enable marine plastic sustainable conversion.

2 Materials and method

2.1 Materials

The present study used virgin plastics and reagent-grade salts for the HTP experiments to understand the contributions of each role. Low-density PE, PP, PET, and nylon 6 (PA), the most common plastics in the sea, were selected in the HTP experiment. Before HTP, these raw plastics were pulverized into ~1 mm powders after being purchased from the Sigma-Aldrich Co., Ltd., USA. The salts imitated the compositions of seawater and included NaCl (AR, > 99%), $MgCl_2$ (AR, > 97%), $MgSO_4$ (AR, > 99%), K_2SO_4 (AR, > 99%), $CaSO_4$ (AR, > 99%), and $CaCO_3$ (AR, > 99%), which were purchased from the Thermo Fisher Scientific Co., Ltd., USA. Deionized water was the liquid phase employed in the tests.

2.2 Data collection

2.2.1 Experimental data

HTP was carried out in a laboratory setting with a 100-mL autoclave reactor without additional gas pressure. Temperature, residence time, plastics/solvent ratio, and solvent density in the reactor were the process parameters to investigate the process efficiency. This work experimented with 80 group tests with different feedstock ratios, salt amounts, and parameters to obtain adequate data for ML analysis. Each test heated the mixture to the desired process temperature in a laboratory oven at approximately 10 $K \cdot min^{-1}$ to the set temperature. After cooling the HTP, filtration of the mixture separated the hydrochar and liquid fraction using Whatman filter paper of 1.2 mm pore size. For subsequent examination, the hydrochar was dried at 105 °C for 24 h before being kept at room temperature. The reservation of the liquid phase was in a PP vessel at 25 °C.

The elemental analysis detected the carbon, hydrogen, nitrogen, and sulfur contents for each sample (original mixture and hydrochar) by using a CHNS analyzer (Perkin-Elmer 2400, UK). In all cases, the initial sample weight was 50 mg and employed sulfamethazine as the internal standard. The mass difference calculated the contents of oxygen. Subsequently, the response data set collected the elemental ratios of H/C, O/C, and N/C as the output data sets.

2.2.2 Literature data collection and screening

The publications regarding plastic hydrothermal conversion supplied partial data sets. Data collection reviewed the HTP literature using PE, PP, PET, or PA as feedstock. Searching keywords involved plastics, PE, PP, PA, PET, hydrothermal carbonization, and hydrochar. With the scope to fit this work, the literature screening only deals with specific plastic conversion in non-catalytic conditions. The collected data sets from relevant publications were summarized along with the experimental as the original data sets and enclosed in the supplementary materials.

2.3 ML algorithms comparisons

In our previous study of plastic thermal conversion, DT, NN, and SVM performed practicable fitness in modeling [17]. Hence, the current work tested three algorithms to fit the HTP process upon the MATLAB software (version 2022b). Their MATLAB functions were fitrensemble, fitrnet, and fitsvm, respectively. Within 87 groups data set, each algorithm divided data sets into a training (70% of total data points) and a validation test (30% of total data points). The modeling process randomly selected the division from the data sets to test the robustness and predictability of the models. Among these supervised ML algorithms, DT uses hyperparameter optimization and pruning to prevent over-fitting and uses the MATLAB function fitrensemble for model development. NN is a system based on the operation of biological NN which analyze data sets and train themselves to recognize patterns between the input variables and responses. It consists of the input and output layers and several hidden layers with adjustable weighted linkages. SVM is an algorithm that transforms a linear programming problem into a dual problem. A kernel function is used to develop the linear relationship between input and response, and the statistical structure risk minimization principle reduced the confidence range to a small genuine risk.

2.4 Techno-economic assessment for the potential process

In addition to the modeling aspect, the techno-economic assessment of the following process meticulously examined the feasibility and economics of the on-ship marine plastics-to-methanol system. The total investment cost encompasses the initial capital outlay, covering direct and indirect expenses, which include equipment procurement, installation, supervision, preliminary engineering design, construction outlays, and startup

costs. Given that this is a mobile on-ship factory, there is no need to factor in land costs, resulting in a proportion of the direct cost savings. Operation and maintenance (O&M) costs are further categorized into fixed and variable components. Fixed O&M costs include expenditures related to salaries, maintenance, insurance, overhead, and taxes, all of which remain constant and are unrelated to the production rate. On the other hand, variable O&M costs are influenced by the production rate and encompass expenses for raw materials, catalysts, and power consumption. This study employed an automated framework developed by Ref. [20] and utilized a reference configuration with a carbon ratio of 85.7 wt %. Detailed assumptions regarding the prices of input and output streams are available in the supplementary materials. A more comprehensive understanding of the calculation framework and assumptions is provided in the Electronic Supplementary Material (ESM).

3 Results and discussion

3.1 Assumption of the marine debris and data statistical analysis

Converting syngas to methanol is widespread in industries such as coal and natural gas, enabling the production of various products like olefins, gasoline, aromatics, and other chemicals across numerous stable-running factories worldwide [21]. Previous studies have demonstrated the feasibility of converting waste polyolefins into syngas, laying the groundwork for subsequent methanol synthesis and successfully investigating them on a modeling scale [22]. This work transitions the process to upcycle ocean plastics, as depicted in Fig. 1(a), involving HTP of marine plastics, followed by an industrial practice for converting treated plastics into methanol. The process begins with pulverizing waste plastics, followed by a float screening to segregate floating and submerged parts. Lighter plastics proceed to subsequent stages, while submerged ones undergo drying and packaging for recycling. HTP allows direct treatment of plastics with seawater without requiring drying or desalination. Generated hydrochar undergoes thermal drying for further gasification and solvent access to a centralized water treatment unit. Steam gasification integrated with methane reforming converts most hydrochar and combusts any unconverted char to supply heat and balance energy. The Rectisol unit purifies gasification products to produce synthesis-level syngas, utilizing chilled methanol to remove impurities and yield a pure syngas stream. A commercial Cu/ZnO/Al_2O_3 catalyst in the synthesis reactor facilitates CO_2 hydrogenation to methanol and the water-gas shift (WGS). Subsequent column purifications refine crudes to produce methanol for use as the Rectisol solvent or the

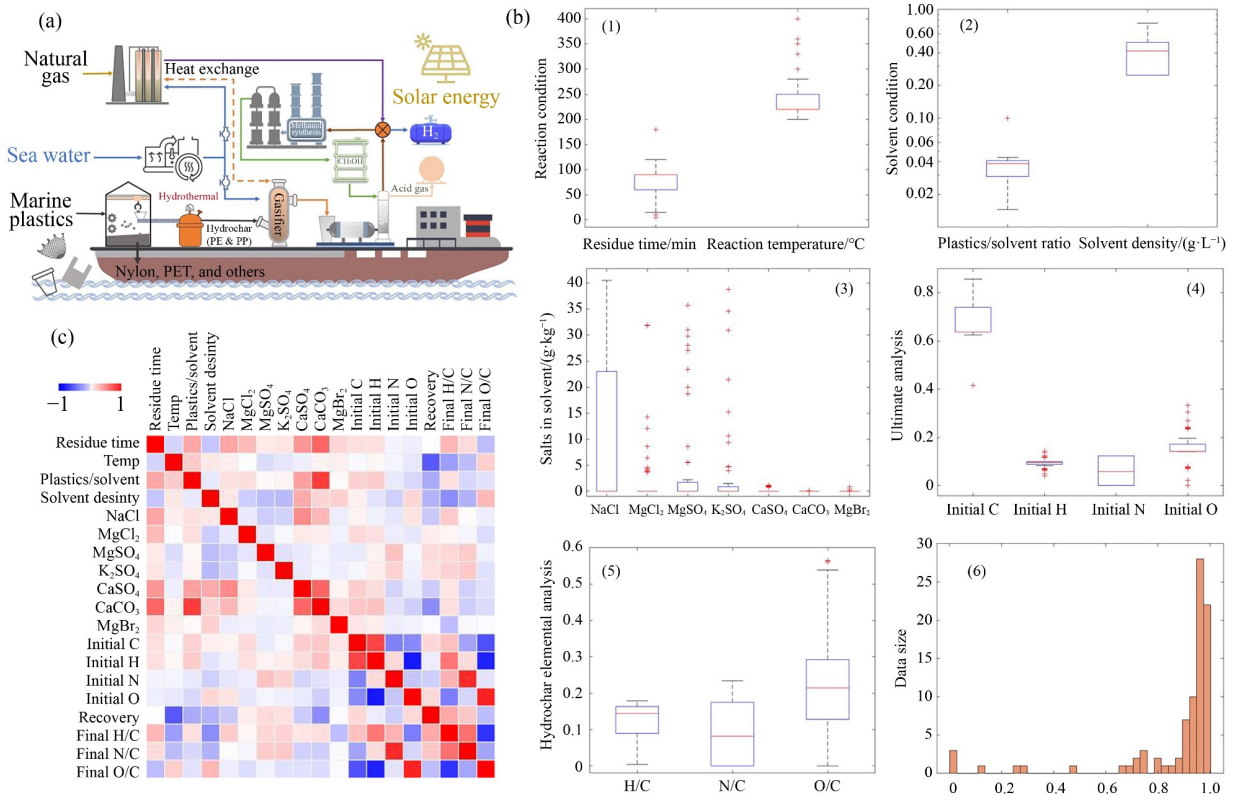

Fig. 1 (a) An overview of the marine debris conversion assumptions, (b) a summary of statistical data for input and response data sets, and (c) a heatmap illustrating data correlations.

final product. The WGS process converts unconverted syngas into hydrogen and storable CO_2, serving as additional products.

Figure 1(b) statistically summarizes input data sets, including salts in the solvent, ultimate analysis, solvent conditions, and reaction conditions. With salts, the total inorganic compounds account for approximately 35 $g \cdot kg^{-1}$ of seawater. The dominant positive ions comprise Na^+, Mg^{2+}, K^+, and Ca^{2+}, and the dominant negative ions include Cl^-, SO_4^{2-}, CO_3^{2-}, and Br^- [23,24]. NaCl is the predominant salt in seawater, with a content of about 22–27 $g \cdot kg^{-1}$, followed by $MgCl_2$, with 2–3 $g \cdot kg^{-1}$ [23,25]. To simulate the salts in the solvent or deposited on the debris, the salt effects studies added several inorganic salts with different concentrations. The addition of NaCl ranges up to 40.5 $g \cdot kg^{-1}$ when pursuing extreme conditions, and the commonly used input was up to 23 $g \cdot kg^{-1}$. As well as the NaCl, the salts with fewer amounts were investigated to reveal the comprehensive effects of the HTP, which consists of $MgCl_2$, $MgSO_4$, K_2SO_4, $CaSO_4$, $CaCO_3$, and $MgBr_2$. Next, ultimate analysis refers to the composition of plastics. Both virgin PE and PP contain carbon and hydrogen elements with ratios of 0.857 and 0.143, respectively, which provide only hydrocarbons to the mixture. Virgin PET has elemental ratios of 0.625 carbon elements, 0.042 hydrogen elements, and 0.333 oxygen elements. Nylon-6, or PA, contains carbon, hydrogen, oxygen, and nitrogen, of which the ratios are 0.637, 0.097, 0.141, and 0.124, respectively, and is the nitrogen source in the mixture. Without considering the pure polyolefin of 0.857, the median carbon ratio ranges from 0.64 to 0.74. A higher carbon ratio refers to more polyolefin in the mixture. Correspondingly, a lower hydrogen ratio refers to less polyolefin, as polyolefin has the most hydrogen elements. Plastic additives, however, also introduce more elemental species when addressing real-world plastics, because of some additives are sulfide, bromide, or phosphide [26]. Notably, this work concentrates on polymer framework conversion in HTP. The results of sulfide and bromide removal could be found in previous reports [15]. The data sets also accounted for solvent effects in statistical results. The plastic-to-solvent ratio runs from 0.0145 to 0.1, with a median of 0.0384, whereas the solvent density is between 0.25 and 0.75. With the reaction conditions, the temperature data set ranges from 200 to 400 °C, and the reaction time is from 5 to 180 min.

In Fig. 1(b), the response data sets (5) and (6) encompass two distinct categories: hydrochar compositions and their recovery yields. Within the hydrochar compositions, essential elemental ratios are considered, including N/C, O/C, and H/C, which provide insights into the chemical properties of the product. Additionally, the response data set accounts for recovery yields and represents the final hydrochar recovery resulting from various input data sets. Among these response data sets, the N/C ratio stands out as particularly significant in the context of HTP for hydrochar gasification. The primary objective of HTP in this study is to eliminate nitrogen from the hydrochar, facilitating the production of pure syngas. Within the range of elemental ratios, the N/C data set varies from 0 to 0.234. Instances with a ratio of 0 indicate partial non-PA conversion, while values above 0 entail complete hydrolysis of PA. Kinetic analysis of hydrothermal PA depolymerization, as reported in previous research [27], provided data sets involving an N/C ratio of zero. This research was conducted at temperatures ranging from 300 to 400 °C, with reaction times spanning 5 to 60 min. The primary products of PA hydrolysis were found to be soluble caprolactam and aminocaproic acid. Initially, PA underwent degradation into aminocaproic acid through hydrolysis, followed by further decomposition into smaller molecules. This observation underscores the importance of addressing wastewater treatment within the current integration system. In addition to the N/C ratio, the ratios of H/C and O/C, along with the recovery yield, play a crucial role in determining the potential productivity of the resulting syngas. Specifically, carbon recovery holds significance, as it theoretically impacts the ultimate syngas yields in a steam gasification process and serves as the exclusive carbon source for subsequent carbon oxide conversion and steam reforming processes.

3.2 Modeling of the hydrochar recovery

Upon the input and response data sets summarized above, three different algorithms, namely DT, NN, and SVM, were employed to assess their suitability in predicting the recovery yields of hydrochar. The evaluation criteria for the model responses included the coefficient of determination (R^2) and the root-mean-squared error (RMSE) for both the trained and tested data sets. For DT modeling, the R^2 value for the training data was notably high at 0.997, but it dropped to 0.787 for the testing data. NN followed closely with an R^2 value of 0.965 for both the training and testing data sets. Additionally, RMSE values were calculated for the training and testing data sets. DT exhibited fewer differences in RMSEs between the training and testing data sets, while NN had higher RMSE values compared to DT for both the training and testing data sets. In contrast to the high accuracies achieved by DT and NN, the SVM algorithm yielded a much lower R^2 value of 0.469 for both the training and testing data sets. Furthermore, the RMSE values for the SVM models were higher than those of the DT and NN models for the data sets. These observations collectively suggest that the SVM algorithm may not be well-suited for modeling in the present work due to its comparatively lower accuracy.

Figure 2(b) displays fitness plots for various responses obtained using the DT algorithm. As previously mentioned, the response data sets for recovery yields range from 0 to 1, with some partial data points

approaching 1 originating from experimental outcomes of ineffectively managed PA and/or PET degradation. The plot illustrates that most training points align closely with the fitness line, but numerous test points fall outside of this line, indicating overfitting within the DT algorithm. Overfitting occurs when a proposed curve attempts to fit all or nearly all data points with zero error, which can be problematic when the proposed curve (model) introduces errors due to noise in the data. Overfitting often arises when a model is excessively accurate or overly complex. While a perfect fit might seem ideal, it may disregard the actual shape of the underlying curve, which can take various forms and often includes some degree of noise. If a model fits all data perfectly without error, it raises questions about whether the proposed result has captured data noise. The DT algorithm, primarily used for classification tasks, typically mitigates overfitting concerns when applied to massive data sets, which allows for higher modeling accuracy [28]. Given the restricted size of the current data set, mitigating overfitting presents a significant challenge, and in practical modeling scenarios, complete avoidance is often challenging.

The predictor importance module within the DT algorithm provided a visual representation of each factor's contribution, as depicted in Fig. 2(b), facilitating a deeper understanding of their impact on the outcome to ascertain the significance of various factors. The classification algorithm of DT was instrumental in revealing the importance of each predictor, enhancing interpretability. While ensemble methods like DT share a black-box nature with NN, tree-based algorithms offer improved interpretability due to their capacity to extract feature importance through a voting mechanism [29]. It was evident that reaction temperature exerted the most substantial influence on hydrochar production from plastic HTP, followed closely by reaction time. These two factors together accounted for 74% of the total importance estimates, underscoring the dominant role of reaction conditions in promoting non-catalytic hydrothermal conversion. Conversely, the initial compositions of the feedstock contributed only 11% to the importance estimates. This observation emphasizes the versatility of hydrothermal digestion, demonstrating its efficacy in processing various organic wastes, including different types of plastics, under optimal reaction conditions. The solvent's impact ranked lowest among all factors, collectively representing a 5% importance estimate, suggesting that solvent density and solid-to-liquid ratio played relatively minor roles in system design. Among the input factors, the influence of NaCl on the response exhibited significant importance, surpassing other salts present in the solvent. This outcome may be attributed to the prevalence of NaCl in seawater, which guided the data collection involving substantial experimental doses. Additionally, this observation implies that excessive salt contamination in the feedstock could impede hydrochar recovery from marine plastics. Consequently, pre-washing is essential when handling plastics heavily contaminated with salt.

Building upon the insights derived from the DT vote

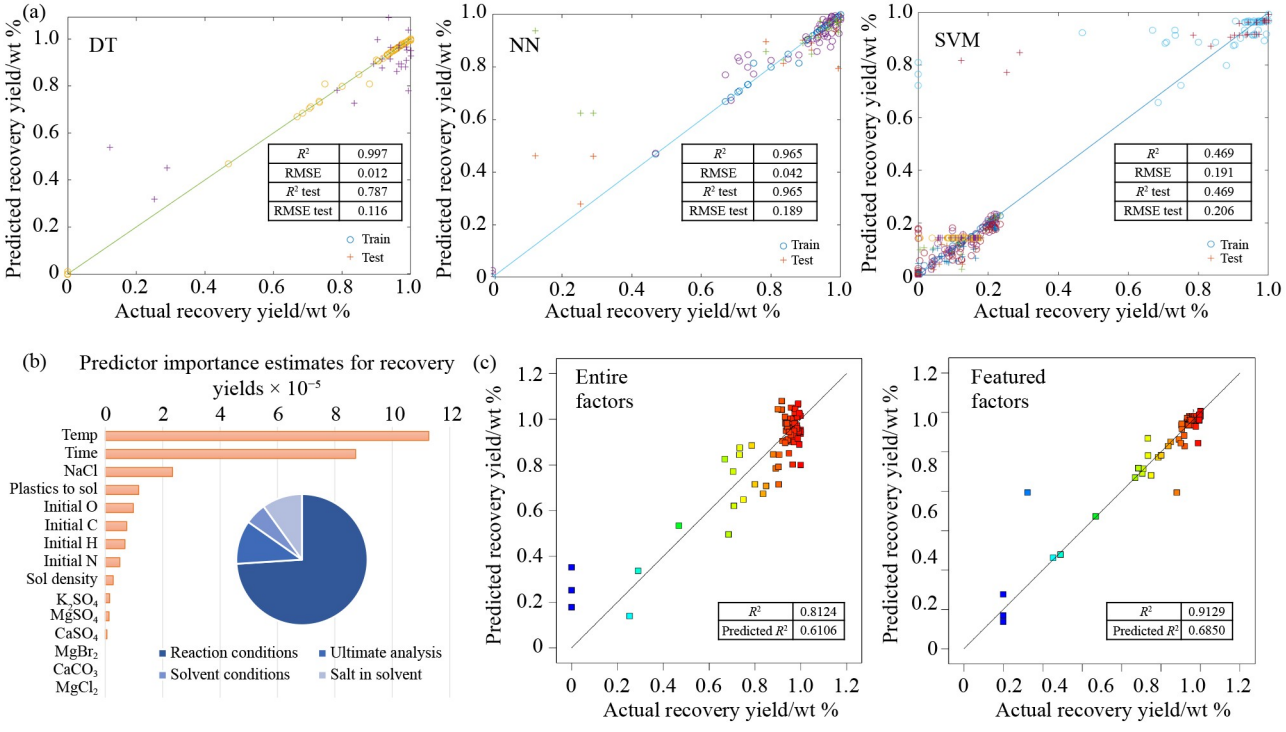

Fig. 2 Regression plots for training and testing using DT, NN, and SVM algorithms for (a) hydrochar recovery modeling, (b) importance estimates for recovery yield predictors, and (c) cross-validation fitness analysis.

analysis mentioned above, Figure 2(c) provides comparative cross-validation results using the complete set of factors and only the featured inputs. When using the complete set for modeling, the cross-validation yielded an R^2 value of 0.8124, with a predicted R^2 of 0.6106. In contrast, focusing on the featured factors, such as reaction temperature, residence time, and NaCl content, for modeling resulted in an R^2 of 0.9129 and a predicted R^2 of 0.6850. This outcome underscores a robust and dependable correlation between recovery rates and reaction conditions, as well as the NaCl content. This strong correlation emphasizes the practicality of hydrochar recovery modeling. While the accuracy of 0.9129 is slightly lower than that achieved with ML approaches, the low cost and satisfactory results make cross-validation a viable choice for practical modeling. Importantly, this approach effectively tackles and mitigates potential overfitting concerns that can arise with algorithms and serves as an assist means to validate the accuracy.

3.3 Modeling of the hydrochar compositions

In hydrochar composition modeling, the DT method was initially employed to forecast elemental composition ratios within the hydrochar, focusing particularly on N/C, O/C, and H/C ratios. Figure 3 showcases the DT algorithm's remarkable precision in predicting these composition ratios. For the training data, it becomes apparent that R^2 values were close to 1 for N/C and H/C, while O/C demonstrated an impressive R^2 of 0.97. However, the test data presented a broader spectrum of R^2 values, ranging from 0.75 to 0.815, suggesting variances in the modeling outcomes associated with this algorithm. When evaluating the test data for H/C, N/C, and O/C ratios, it becomes evident that the fits obtained are suboptimal, as substantiated by R^2 values of 0.794, 0.75, and 0.815, respectively. Furthermore, the presence of noticeable RMSE values in these predictions underscores the need to enhance the accuracy of elemental composition ratio forecasts within hydrochar. These findings imply the possibility of overfitting during the modeling process, warranting further investigation to rectify these discrepancies and improve model performance.

Furthermore, the DT algorithms provide informative estimating hydrochar compositions, as depicted in Fig. 3(b). A common thread among the factors influencing hydrochar composition ratios was the substantial contribution of initial compositions. Ultimate analysis played a significant role, accounting for 78%, 74%, and 63% of the estimates for O/C, N/C, and H/C ratios in hydrochar, respectively. Specifically, the initial presence of H, C, and O drove the O/C ratio in hydrochar, while the initial N content primarily influenced the N/C ratio, and initial H and O content had a notable impact on the H/C ratio. The introduction of O or N in polymers replaced some of the existing C and H, resulting in the decline of their respective ratios within the polymer structure. Notably, ultimate analysis had a different level of importance for hydrochar H/C compared to O/C and N/C. Additionally, the NaCl content in the system also played a role in influencing the H/C ratio. This observation can be attributed to the hydrolysis of materials like PA and PET, which led to a reduction in H content through the breaking of amide and ester bonds. As discussed earlier, lower NaCl content facilitated higher hydrochar recovery, and experimental results supported

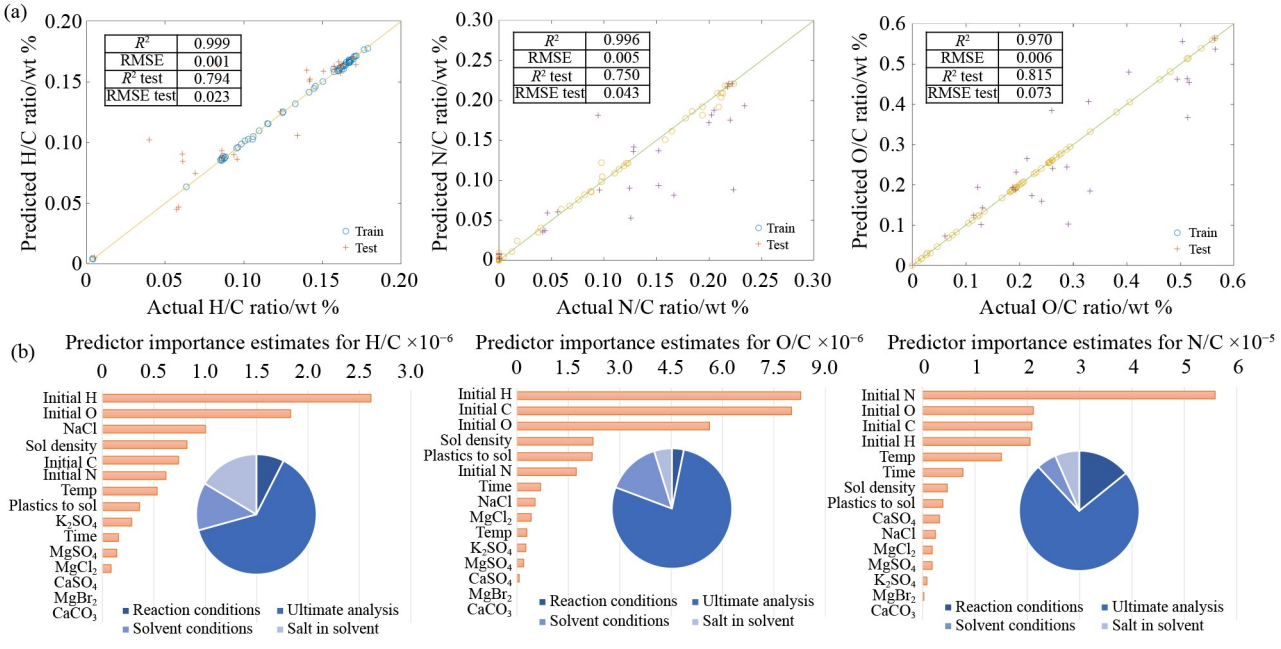

Fig. 3 (a) Regression plots for training and testing using the DT algorithm for hydrochar composition modeling, (b) importance estimates for predictors of each hydrochar composition derived from the DT algorithm.

this observation, particularly in the case of PA hydrolysis. The predictor importance estimates provided valuable insights into the factors influencing hydrochar formation, particularly when aiming for high recovery yields. To optimize the HTP model for hydrochar gasification, primary considerations should focus on the reaction conditions, initial elemental compositions (to replace plastic qualitative analysis), and the NaCl content in the solvent. The reaction conditions and NaCl content primarily determined hydrochar yield, while the initial elemental composition content influenced hydrochar purity. The interplay between initial elemental composition and NaCl content jointly influenced the H/C ratio in hydrochar.

As depicted in Fig. 4, this study also conducted a comparative analysis of NN and SVM, two commonly employed algorithms, to predict the elemental composition of hydrochar. The NN algorithm, serving as a secondary approach for composition ratio predictions, exhibited remarkable accuracy with R^2 values exceeding 0.936 for N/C and O/C, and achieving 0.817 for H/C, underscoring its proficiency in hydrochar modeling aspect. In contrast to the DT algorithm, which demonstrated a perfect fit with the training data sets, the NN algorithm yielded acceptable results when applied to both the training and test data sets. However, the gap between the training and test data sets for each response was considerably smaller than that observed with DT-modeled results. This outcome suggests that NN may have established more practical models than DT. It's worth noting that NN is an information processing structure, particularly suited for applications with unbounded activation functions [30]. The NN can be configured or trained to address specific problems, including classification tasks. It learns from extensive sets of feature vectors, which are accompanied by pre-configured classes or labels, making it a versatile tool for various applications [31]. In the aspect of polymer degradation predictions, tree-based algorithms have historically been less frequently utilized than NN [32]. Some practices resorted to collecting extensive training data sets to mitigate the overfitting issues associated with tree-based algorithms. However, when comparing ANN and tree-based algorithms for pyrolysis composition prediction, they were found to achieve similar levels of prediction accuracy [33]. In practical scenarios, the choice of a ML model depends on the desired level of accuracy and the availability of training data. Considering these factors, the ANN algorithm holds several advantages and appears well-suited for addressing the objectives of the current research.

The SVM modeling results reveal a lack of accuracy and reliability in the predictions. The H/C ratio exhibits a notably weak fit, with an R^2 value of 0.651 and an elevated RMSE of 0.054. These deficiencies persist in the test data, where the R^2 remains low at 0.651, and the RMSE, though slightly improved at 0.045, still signifies substantial prediction errors. Similarly, the N/C ratio presents challenges, with an R^2 of merely 0.31 and an RMSE of 0.047, indicating significant uncertainties in the

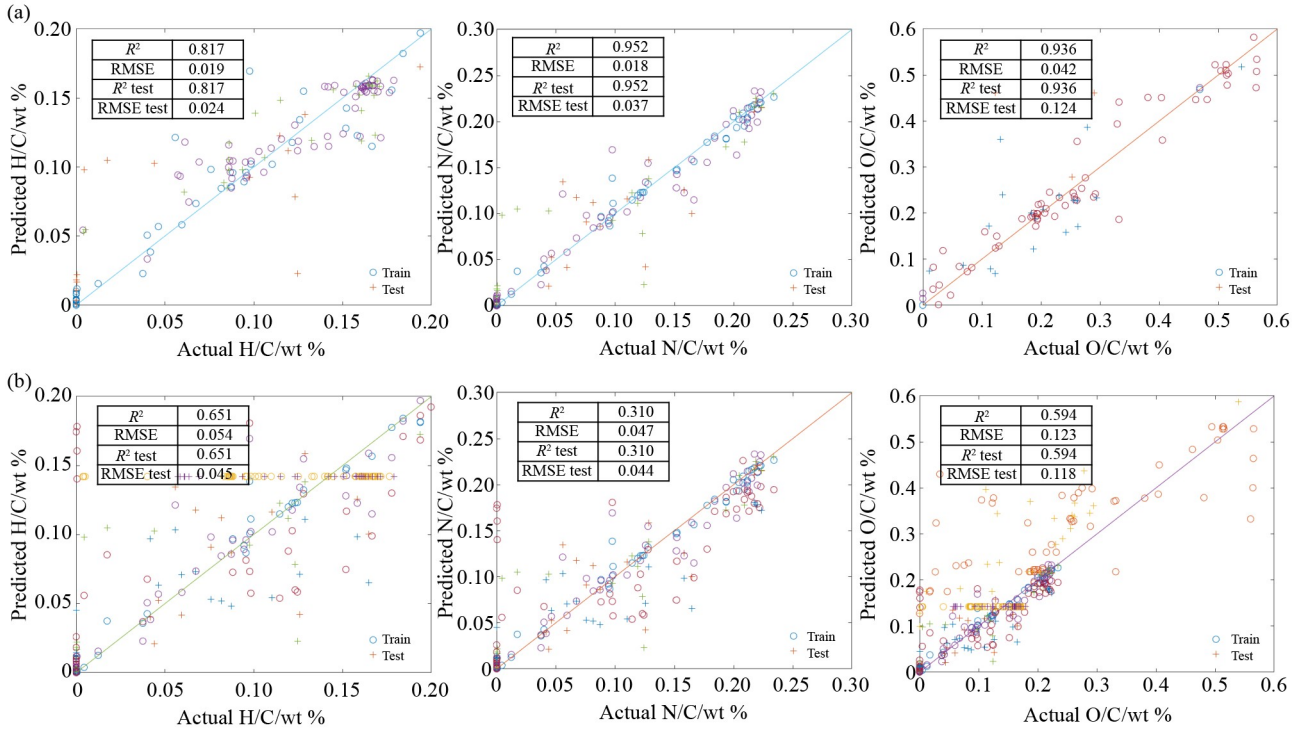

Fig. 4 Regression plots illustrating training and testing results for hydrochar composition modeling using (a) the NN algorithm and (b) SVM algorithm.

predictions. These issues persist in the test data, where the R^2 remains equally low at 0.31, and the RMSE stands at 0.044. While the O/C ratio achieves a relatively higher R^2 of 0.594, the RMSE remains at 0.123, with considerable prediction errors. These challenges also extend to the test data, with an R^2 of 0.594 and an RMSE of 0.118. Collectively, these outcomes highlight the necessity for substantial enhancements to improve the reliability of these predictions. It's worth noting that SVM is typically recognized for its binary classification capabilities in regression, where the hyperplane serves as the prediction line for target values. SVM defines boundary lines around the hyperplane to create margins containing observed values. Support vectors play a pivotal role in defining the hyperplane within SVM, with the aim of encompassing as many data points as possible within the boundary lines. This strategy serves to maximize the fit of data points within these margins. In certain contexts, such as predicting plastic pyrolysis, SVM and ANN methods have demonstrated the ability to model gas and liquid yields in both procedures with a remarkable 99% accuracy [34]. Additionally, SVM models have successfully predicted hydrogen yield with an impressive R^2 value of 0.997 when estimating hydrogen yield in biomass gasification [35]. However, a significant drawback of SVM, the quadratic programming problem (QPP), is inevitable. This computational challenge can be particularly cumbersome in training classifiers [36]. Furthermore, when dealing with extensive data sets, as illustrated in Section 3.1, which involves input factors related to marine debris conversion encompassing 15 items, SVM's computational demands increase substantially, and vast data sets would make QPP solving unworkable [37]. Its heightened computational complexity may offer insights into the observed reduced accuracy in the SVM algorithm within this study.

3.4 Featured factors for hydrochar composition modeling with NN algorithm

The NN algorithm has demonstrated satisfactory performance in hydrochar composition modeling, particularly for the N/C and O/C ratios. However, further optimization of featured factors is necessary to enhance accuracy and cost-efficiency in modeling. Figure 5(a) illustrates the hydrochar composition modeling using the NN algorithm with these featured factors. Leveraging insights from the DT vote analysis, tailored featured sets, comprising the top 7, 6, and 5 factors for the H/C, O/C, and N/C composition ratios, respectively, were utilized in hydrochar composition modeling. Specifically, the model for the H/C ratio demonstrated a robust fit, with both R^2 and R^2 test values of 0.9376, along with an exceptionally low RMSE of 0.0113, signifying minimal prediction errors. This observation is better than using full factor set modeling, of which R^2 was 0.817. However, in the cases of O/C and N/C, featured sets showed worse performance than the full set. The modeling of the O/C ratio yielded an R^2 value of 0.9027 and an RMSE of 0.0499. For the test data, the R^2 value remained at 0.9027, and the RMSE decreased to 0.0368. Regarding the N/C ratio, the model provided an R^2 value of 0.8353 and an RMSE of 0.0364. These findings were consistent in the test data, with an R^2 value of 0.8353 and a reduced RMSE of 0.0332.

Figure 5(b) presents a comparative cross-validation with full factors set by showcasing hydrochar

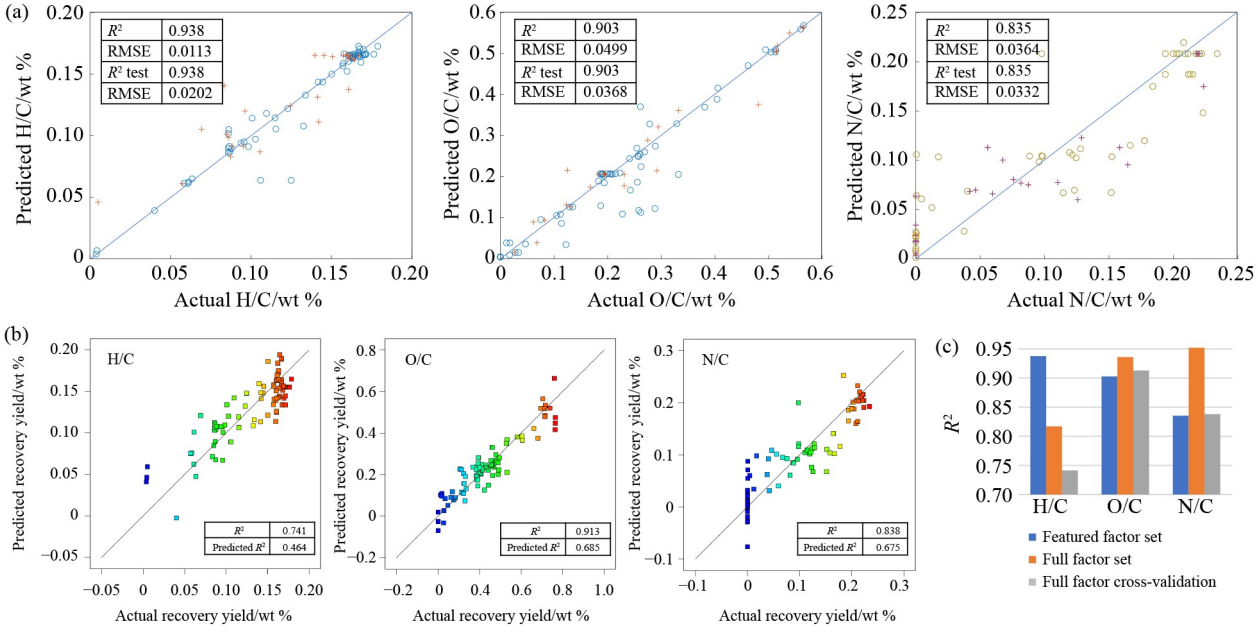

Fig. 5 Regression plots illustrating (a) training and test data with the NN algorithm for hydrochar composition modeling using featured factors sets, (b) cross-validation results for hydrochar compositions with full factors set, and (c) a summary of R^2 values.

composition modeling using the NN algorithm. The results reveal varying levels of accuracy and predictive performance across different elemental composition ratios. For the H/C ratio, the model achieved an R^2 of 0.7414, indicating a moderate fit, but the predicted R^2 of 0.4642 suggests a decrease in predictive reliability. In the case of the O/C ratio, the model demonstrated a high level of accuracy with an R^2 of 0.9129, and the predicted R^2 remained respectable at 0.685. Finally, for the N/C ratio modeling, an R^2 of 0.838 signified good predictive performance, with a predicted R^2 of 0.6754. These findings highlight the model's variable performance when predicting different elemental composition ratios in hydrochar modeling with featured factors.

Figure 5(c) compiles R^2 outcomes for hydrochar composition modeling, evaluating the effectiveness of multiple configurations across different elemental composition ratios (H/C, O/C, N/C), encompassing the utilization of the NN algorithm with featured and full factor sets, and cross-validation with complete factor sets. For the H/C ratio prediction, the NN with the featured factor set serves optimal, yielding an R^2 of 0.938, emblematic of a robust model with minimal prediction errors. In contrast, the full-factor models fall slightly short in predictive accuracy. Moving to the O/C ratio prediction, the full factor set using the NN algorithm delivers an accurate model with an R^2 of 0.936, establishing its reliability in forecasting this ratio. Meanwhile, the NN algorithm with the featured factor set and cross-validation with full factor set, although slightly lower with R^2 values of 0.903 and 0.913, respectively, remain competitive options, offering flexibility in model selection. The N/C ratio prediction reveals that the full factor set excels with an R^2 of 0.952, indicating decent accuracy, which is higher than the featured factor set of 0.835. Consequently, the model configuration should align with the specific elemental composition ratio of interest. While the featured factor set generally demonstrates superior performance for the H/C ratio, the full factor set shines when predicting the O/C and N/C ratios.

3.5 Potential of the following process

Previous research has established the viability of converting waste plastics into syngas, facilitating subsequent processes [38,39]. This study focuses on assessing the feasibility of the following process with the assumption of shipboard accessibility. The conceptual design integrates a pretreatment unit to prepare plastics for gasification. The current study assumes onboard equipment requires no significant or costly modifications. Regarding the collection of widely dispersed debris, collaborative efforts led by groups, such as Ocean Cleanup, are assumed to address this aspect. Thus, this study presumes the availability and collectability of such debris. In addition, this research seeks to assess the feasibility of establishing similar plastic-to-methanol facilities on ships, drawing insights from studies that have conducted techno-economic evaluations of land-based installations [39]. The study compared an example based on a land-based plant capable of processing 2500 $kg \cdot h^{-1}$ of plastic. According to the data from 2010, approximately 275 million metric tons of plastic waste were generated in 192 coastal countries, with an estimated 4.8 to 12.7 million metric tons eventually entering the ocean [2]. It underscores the need to deploy multiple such plants, operating for decades, to combat plastic pollution in a specific ocean area.

In recent years, the global methanol price has exhibited fluctuations spanning from 0.19 to 0.54 $€ \cdot kg^{-1}$, with detailed information available in the supplementary materials. To simplify this study, a median price of 0.34 $€ \cdot kg^{-1}$ is utilized to compute methanol revenues. In the comparative evaluation of plastics-to-methanol processes, the conventional gasification-synthesis method incurred a cost of 0.53 $€ \cdot kg^{-1}$. However, an integrated system that includes methane reforming achieved a considerably reduced cost of 0.26 $€ \cdot kg^{-1}$ [38]. This cost reduction holds appeal for on-ship facilities, as they can tap into abundant marine natural gas resources with relatively economical transportation expenses. Moreover, the process exhibits the potential to attain nearly net-zero emissions by efficiently capturing carbon dioxide during syngas generation while simultaneously releasing energy. Given the plant's focus on plastic waste in remote oceanic regions, optimizing the utilization of marine resources and minimizing production costs becomes imperative. As a result, this study integrates natural gas reforming into the system to enhance its economic viability and environmental sustainability.

Table 1 presents an economic comparison between a land-based and an on-ship factory for methanol production from waste, with assumptions drawn from previous reports [39]. The table examines various input factors required for production, including oxygen, natural gas, and demi-water, as well as the resulting product streams of methanol and carbon dioxide. The results indicate that the on-ship factory exhibits greater cost-effectiveness than the land-based facility. This advantage is attributed to the onboard infrastructure, which efficiently manages water treatment through a centralized system and harnesses cost-effective power from abundant solar energy using photovoltaic devices. However, it's worth noting that the land-based factory in a specific region generates a higher net revenue than the on-ship factory. This is primarily due to the land-based facility receiving waste disposal fees from domestic organizations [39].

The capital expenditure calculations were based on the methodology outlined by previous report [20], utilizing a CEPCI value of 813 for 2022. It resulted in total module cost, grass roots cost, and working capital estimates of 14876948.78, 19531047.77, and 2929657.16 €,

respectively. As depicted in Fig. 6, the methanol price has exhibited significant fluctuations over the past decade, suggesting that the payback period for a single plant varies from 3 to 7 yr, depending on the methanol price, which ranges from 0.27 to 0.46 €·kg^{-1}. It's worth emphasizing that, when considering equivalent methanol productivity at the same scale, the payback period for an on-ship factory tends to be more durable than that of a land-based facility. This analysis, however, takes no safety aspect into account. Implementing safety measures on a ship is notably more complex than on land, requiring a reduced feeding rate to ensure safe and secure operations. Despite the mobility advantages that can lead to reduced transportation costs and improved profitability through innovative sales models, it's notable to acknowledge that scale remains a fundamental factor influencing overall profitability. Therefore, the payback time for a smaller-scale factory would likely be even longer. This apparent contradiction underscores the need for future integration efforts to optimize the scale and explore hybrid approaches, such as a partial on-ship setup combined with a land-based factory on an island, in pursuit of a balanced and economically viable solution.

4 Conclusions

This study extensively investigated hydrochar composition modeling by employing advanced algorithms and rigorous analyses to uncover insights into elemental composition ratios of hydrochar, comprehend the factors influencing hydrochar compositions, and contribute to optimizing hydrochar production processes. The hydrochar recovery modeling begins with the DT algorithm,

Table 1 The economic estimations of waste to methanol factories

Streams	Unit	Land-based	Shipboard
Input			
Oxygen consumption	kg·h^{-1}	2057	2057
Oxygen cost	€·h^{-1}	287.98	275.1
Natural gas consumption	kg·h^{-1}	272.3	272.3
Natural gas cost	€·h^{-1}	25.052	27.674
Demi-water consumption	kg·h^{-1}	1856	1856
Demi-water cost	€·h^{-1}	10.208	13.552
Dlectricity consumption	kWh	1227	1227
Electricity cost	€·h^{-1}	146.43	39.005
Total costs	€·h^{-1}	469.67	355.331
Output			
Methanol yield	99.98% w/w, kg·h^{-1}	3181	3181
Methanol revenues	€·h^{-1}	1081.54	1045.84
CO_2	99% w/w, kg·h^{-1}	1977	1977
CO_2 revenues	€·h^{-1}	120.597	150.975
Plastic disposal fee	€·h^{-1}	172.5	0
Total revenues	€·h^{-1}	1374.64	1196.815
Operative margin	€·h^{-1}	904.967	841.484

Fig. 6 The methanol price tendency in the past decade and estimated payback years.

which effectively captures relationships between initial compositions and hydrochar ratios but faces limitations in predictive accuracy due to overfitting. However, the DT vote analysis identifies reaction conditions and NaCl as pivotal factors for recovery, making low-cost featured factors cross-validation a practical choice for recovery modeling. Subsequently, various algorithms are compared to predict hydrochar composition ratios. The NN algorithm achieves R^2 values exceeding 0.936 for N/C and O/C, and 0.817 for H/C, indicating potential for generalization. Notably, when paired with featured factors, the NN algorithm significantly enhances model accuracy, particularly for the H/C ratio, with an impressive R^2 of 0.9376. The featured factor set excels in predicting the H/C ratio, while the full factor set performs exceptionally well in O/C and N/C ratios. The study also explores the economic potential of hydrochar production for marine plastics-to-methanol process. Methanol price fluctuations over a decade yield varying payback periods, ranging from 3.3 to 7 yr for hydrochar production plants. On-ship factories demonstrate greater resilience than land-based facilities, capitalizing on marine natural gas resources and the potential for near net-zero emissions.

Competing interests The authors declare that they have no competing interests.

Acknowledgements The authors are grateful for financial support from the Marie Skłodowska Curie Actions Fellowships by The European Research Executive Agency, Belguim (Grant Nos. H2020-MSCA-IF-2020 and 101025906). More importantly, Dr. Yi Cheng acknowledge Dr. Fanhua Kong from the Petrochemical Research Institute of PetroChina Co., Ltd., China, who proposed the initial assumption of the system and years of guidance in the industrial syngas research area.

Electronic Supplementary Material Supplementary material is available in the online version of this article at https://doi.org/10.1007/s11705-024-2468-3 and is accessible for authorized users.

References

1. Sheridan H, Johnson K, Capper A. Analysis of international, European and Scot's law governing marine litter and integration of policy within regional marine plans. Ocean and Coastal Management, 2020, 187: 105119
2. Jambeck J R, Geyer R, Wilcox C, Siegler T R, Perryman M, Andrady A, Narayan R, Law K L. Plastic waste inputs from land into the ocean. Science, 2015, 347(6223): 768–771
3. Pabortsava K, Lampitt R S. High concentrations of plastic hidden beneath the surface of the Atlantic Ocean. Nature Communications, 2020, 11(1): 4073
4. van Giezen A, Wiegmans B. Spoilt-Ocean Cleanup: alternative logistics chains to accommodate plastic waste recycling: an economic evaluation. Transportation Research Interdisciplinary Perspectives, 2020, 5: 100115
5. Yao Z, Ma X. A new approach to transforming PVC waste into energy via combined hydrothermal carbonization and fast pyrolysis. Energy, 2017, 141: 1156–1165
6. Moore C J. Synthetic polymers in the marine environment: a rapidly increasing, long-term threat. Environmental Research, 2008, 108(2): 131–139
7. Martins J, Sobral P. Plastic marine debris on the Portuguese coastline: a matter of size? Marine Pollution Bulletin, 2011, 62(12): 2649–2653
8. Jung M R, Balazs G H, Work T M, Jones T T, Orski S V, Rodriguez C V, Beers K L, Brignac K C, Hyrenbach K D, Jensen B A, et al. Polymer identification of plastic debris ingested by pelagic-phase sea turtles in the central Pacific. Environmental Science & Technology, 2018, 52(20): 11535–11544
9. Hou Q, Zhen M, Qian H, Nie Y, Bai X, Xia T, Laiq Ur Rehman M, Li Q, Ju M. Upcycling and catalytic degradation of plastic wastes. Cell Reports. Physical Science, 2021, 2(8): 100514
10. Lopez G, Artetxe M, Amutio M, Alvarez J, Bilbao J, Olazar M. Recent advances in the gasification of waste plastics. A critical overview. Renewable & Sustainable Energy Reviews, 2018, 82: 576–596
11. Al-Salem S M, Antelava A, Constantinou A, Manos G, Dutta A. A review on thermal and catalytic pyrolysis of plastic solid waste. Journal of Environmental Management, 2017, 197: 177–198
12. Li J, Suvarna M, Pan L, Zhao Y, Wang X. A hybrid data-driven and mechanistic modelling approach for hydrothermal gasification. Applied Energy, 2021, 304: 117674
13. Li J, Pan L, Suvarna M, Wang X. Machine learning aided supercritical water gasification for H_2-rich syngas production with process optimization and catalyst screening. Chemical Engineering Journal, 2021, 426: 131285
14. Raikova S, Knowles T D J, Allen M J, Chuck C J. Co-liquefaction of macroalgae with common marine plastic pollutants. ACS Sustainable Chemistry & Engineering, 2019, 7(7): 6769–6781
15. Iñiguez M E, Conesa J A, Fullana A. Hydrothermal carbonization of marine plastic debris. Fuel, 2019, 257: 116033
16. Ge S, Shi Y, Xia C, Huang Z, Manzo M, Cai L, Ma H, Zhang S, Jiang J, Sonne C, et al. Progress in pyrolysis conversion of waste into value-added liquid pyro-oil, with focus on heating source and machine learning analysis. Energy Conversion and Management, 2021, 245: 114638
17. Cheng Y, Ekici E, Yildiz G, Yang Y, Coward B, Wang J. Applied machine learning for prediction of waste plastic pyrolysis towards valuable fuel and chemicals production. Journal of Analytical and Applied Pyrolysis, 2023, 169: 105857
18. Zhao S, Li J, Chen C, Yan B, Tao J, Chen G. Interpretable

machine learning for predicting and evaluating hydrogen production via supercritical water gasification of biomass. Journal of Cleaner Production, 2021, 316: 128244

19. Katongtung T, Onsree T, Tippayawong N. Machine learning prediction of biocrude yields and higher heating values from hydrothermal liquefaction of wet biomass and wastes. Bioresource Technology, 2022, 344: 126278
20. Prifti K, Galeazzi A, Barbieri M, Manenti F. A Capex Opex Simultaneous Robust Optimizer: Process Simulation-based Generalized Framework for Reliable Economic Estimations. Montastruc L, Negny SBTCACE, eds. Computer Aided Process Engineering, 2022, 51: 1321–1326
21. Olah G A. Beyond oil and gas: the methanol economy. Angewandte Chemie International Edition, 2005, 44(18): 2636–2639
22. Al-Qadri A A, Ahmed U, Abdul Jameel A G, Zahid U, Usman M, Ahmad N. Simulation and modelling of hydrogen production from waste plastics: technoeconomic analysis. Polymers, 2022, 14(10): 2056
23. Besson P, Degboe J, Berge B, Chavagnac V, Fabre S, Berger G. Calcium, Na, K and Mg concentrations in seawater by inductively coupled plasma-atomic emission spectrometry: applications to IAPSO seawater reference material, hydrothermal fluids and synthetic seawater solutions. Geostandards and Geoanalytical Research, 2014, 38(3): 355–362
24. Millero F J, Feistel R, Wright D G, McDougall T J. The composition of standard seawater and the definition of the reference-composition salinity scale. Deep-sea Research. Part I, Oceanographic Research Papers, 2008, 55(1): 50–72
25. Lyman J, Fleming R H. Composition of sea water. Journal of Marine Research, 1940, 3(2): 134–146
26. Wensing M, Uhde E, Salthammer T. Plastics additives in the indoor environment—flame retardants and plasticizers. Science of the Total Environment, 2005, 339(1–3): 19–40
27. Iwaya T, Sasaki M, Goto M. Kinetic analysis for hydrothermal depolymerization of nylon 6. Polymer Degradation & Stability, 2006, 91(9): 1989–1995
28. Hastie J, Tibshirani R, Friedman J. The Elements of Statistical Learning. New York: Springer, 2009
29. Karabadji N E I, Seridi H, Bousetouane F, Dhifli W, Aridhi S. An evolutionary scheme for decision tree construction. Knowledge-Based Systems, 2017, 119: 166–177
30. Clare A, King R D. Knowledge discovery in multi-label phenotype data. In: European conference on principles of data mining and knowledge discovery. Berlin: Springer, 2001, 42–53
31. Boucheron S, Bousquet O, Lugosi G. Theory of classification: a survey of some recent advances. ESAIM: Probability and Statistics, 2005, 9: 323–375
32. Ascher S, Watson I, You S. Machine learning methods for modelling the gasification and pyrolysis of biomass and waste. Renewable & Sustainable Energy Reviews, 2022, 155: 111902
33. Elmaz F, Yücel Ö, Mutlu A Y. Predictive modeling of biomass gasification with machine learning-based regression methods. Energy, 2020, 191: 116541
34. Mighani M, Shahi A, Antonioni G. Catalytic pyrolysis of plastic waste products: time series modeling using least square support vector machine and artificial neural network. In: the 16th International Conference on Sustainable Energy Technologies, 2017, available at WSSET
35. Ozbas E E, Aksu D, Ongen A, Aydin M A, Ozcan H K. Hydrogen production via biomass gasification, and modeling by supervised machine learning algorithms. International Journal of Hydrogen Energy, 2019, 44(32): 17260–17268
36. Fu C, Guo C Y, Lin X R, Liu C C, Lu C J. Tree decomposition for large-scale SVM problems. In: Proceedings of the International Conference on Technologies and Applications of Artificial Intelligence. IEEE, 2010, 11: 233–240
37. Cervantes J, García Lamont F, López-Chau A, Rodríguez Mazahua L, Sergio Ruíz J. Data selection based on decision tree for SVM classification on large data sets. Applied Soft Computing, 2015, 37: 787–798
38. Al-Qadri A A, Ahmed U, Jameel A G, Ahmad N, Zahid U, Zein S H, Naqvi S R. Process design and techno-economic analysis of dual hydrogen and methanol production from plastics using energy integrated system. International Journal of Hydrogen Energy, 2023, 48(29): 10797–10811
39. Prifti K, Galeazzi A, Manenti F. Design and simulation of a plastic waste to methanol process: yields and economics. Industrial & Engineering Chemistry Research, 2023, 62(12): 5083–5096